

Role of hydroxyl groups for the O₂ adsorption on CeO₂ surface: A DFT + *U* study

Hui-Lung Chen^a, Hsin-Tsung Chen^{b,*}

^a Department of Chemistry, Institute of Applied Chemistry, Chinese Culture University, Taipei 111, Taiwan

^b National Center for High-Performance Computing, 28 Nan-Ke 3rd Road, Hsinshi, Tainan 74147, Taiwan

ARTICLE INFO

Article history:

Received 18 March 2010

In final form 17 May 2010

Available online 21 May 2010

ABSTRACT

Our calculations with spin-polarized density functional theory and on-site Coulomb interactions (DFT + *U*) have showed that (i) OH groups can facilitate O₂ adsorption on CeO₂ even at low OH coverages; (ii) the OH groups possess a long-range and coverage effects on the O₂ adsorption; and (iii) the adsorbed O₂ can readily diffuse along the surface Ce atoms in the presence of OH groups, and this may be a large O₂ supply for CO oxidation on the interface of noble-metal/CeO₂. We provide the evidence that O₂ is supplied by superoxide species on CeO₂ in the presence of OH and can diffuse to the interface of noble-metal/CeO₂ for CO oxidation.

© 2010 Elsevier B.V. All rights reserved.

1. Introduction

Highly dispersed noble-metal supported on metal oxide have been shown to efficiently promote low-temperature oxidation of CO [1]. The activity of these catalysts is controlled by several factors, most notably the size of the metal cluster and the presence of metal ions (the oxidation state of metal), often nucleated at surface defects, as well as the ability of the support to supply reactive oxygen, effectively acting as oxygen buffers during the reaction. Ceria (CeO₂) is one of the most efficient reducible oxides which represent very active catalytic supports due to its oxygen storage capacity [2]. Therefore, to obtain insight into CO oxidation on noble-metal/CeO₂ is of great importance. In addition, water molecules inevitably exist in any real catalytic system, and have been found that have a significant effect in the many chemical systems. As a result, the nature of the active sites on noble-metal/CeO₂ catalysts and the mechanisms for CO oxidation are still subjects of debate. Thus, to gain the physical origin of water effect on CO oxidation on noble-metal/CeO₂ is not only essential to understand a comprehensive reaction mechanism, but also fundamental in heterogeneous catalysis in general.

The CO oxidation mechanism has been long concerned. At high temperatures ($T > 500$ °C), oxidation reactions involve lattice oxygen resulting in surface reduction with O vacancy formation, while at low temperatures ($T < 200$ °C) surface oxygen adspecies are involved [3]. However, there is evidence that O₂ cannot adsorb on the perfect CeO₂ surface, but can strongly bind at oxygen vacancies [4–7]. One should note that if vacancies are healed, O₂ would not adsorb on the CeO₂ surface. Therefore, one of the greatest puzzles in the field is: where does O₂ come from for the reaction at the noble-metal/CeO₂ interface? Considering that the CO oxidation

occurs at very low temperature, the O₂ supply may well be the bottleneck for the whole process. There have been extensive experimental studies [8,9], which showed that water plays an important role in CO oxidation. In this study, we aim to address the following questions by using the density functional theory: (i) where is the O₂ reservoir for CO oxidation on the noble-metal/CeO₂? (ii) Does water facilitate the O₂ adsorption on the surface? If yes, what is the role of water? (iii) Could O₂ diffuse to the active interfacial region?

2. Computational methods

The spin-polarized density functional theory (DFT) calculations with the projector augmented wave (PAW) method [10,11] were carried out as implemented in Vienna ab initio simulation package (VASP) [12–16]. The generalized gradient approximation with Perdew–Wang 1991 exchange–correlation functional (GGA-PW91) [17,18] was used. The kinetic cutoff energy for a plane wave basis set was 400 eV. The Brillouin zone was approximated with finite sampling of $3 \times 3 \times 1$ special *k*-points using the Monkhorst–Pack scheme [19]. In this study, the DFT with on-site Coulomb interactions (DFT + *U*) [20] were considered to accurately correct the strong on-site Coulomb repulsion of Ce_{4f} states. The issues with regard to DFT + *U* and the selected value of *U* parameters have been discussed extensively [21–25]. However, there is no general rule on a ‘correct’ *U* value to describe the localized 4f orbitals of Ce. The proposed *U* values seem to depend on the oxidation states of Ce and the functional used. For example, Loschen et al. proposed a well-balanced *U* value of 5–6 eV for LDA + *U* calculations and 2–3 eV for GGA + *U* calculations [24]. Andersson et al. also clarified that the *U* value must satisfy the criteria of $U > 6$ eV for LDA calculations and $U > 5$ eV for GGA calculations to exactly predict the ground state of Ce₂O₃ [23]. As such, we therefore chose $U = 5$ eV

* Corresponding author. Fax: +886 6 505 5909.

E-mail address: htchen@nchc.org.tw (H.-T. Chen).

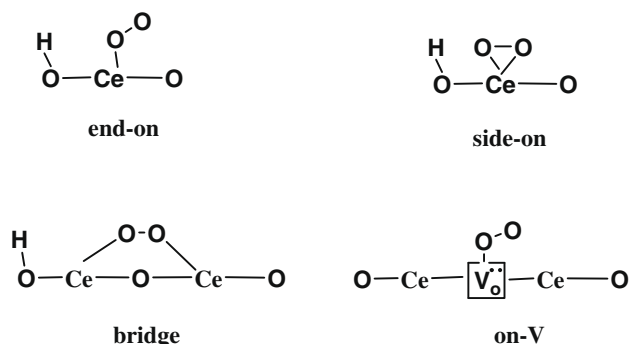
in the present study. To ensure the validity of the computational method, we calculated the lattice parameters and density of states for bulk CeO₂. The effect of the U value on lattice constant is depicted in Fig. S1. The lattice constant of the CeO₂ bulk was calculated to be 5.436 Å at $U = 5$ eV, which is in good agreement with the experimental value of 5.411 Å [26]. The calculated energy gaps of O_{2p} → Ce_{4f} and O_{2p} → Ce_{3d} are 2.3 and 5.6 eV, respectively, which are consistent with the experiment data [26] of 2.54–3.0 and 6.0 eV. The slab models were applied to study the interaction of O₂ on the CeO₂(1 1 1) and (1 1 0) surface, respectively. A nine-layer (1 1 1) and six-layer (1 1 0) supercell were considered, as shown in Fig. S2 and S3. Both slabs were separated by a vacuum space of 15 Å to avoid the interaction force between the upper and the lower slabs. All calculations were carried out by relaxing the adsorbed molecule and the top-three layers of (1 1 1) and (1 1 0) surfaces. The unrelaxed layers were set to estimated bulk parameters. In this study, we calculated the adsorption energies according to

$$\Delta E_{\text{ads}} = -(E_{\text{total}} - E_{\text{surface}} - E_{\text{molecule}})$$

where E_{total} indicates the total energy of adsorbed species on the surface, E_{surface} is the energy of the clean surface, and E_{molecule} is the energy of a gas-phase molecule. Vibrational frequencies of the adsorbed structures were analyzed by diagonalizing the Hessian matrix of selected atoms within the VASP approach. The nudged elastic band (NEB) method [27–29] is applied to locate transition states, and minimum energy pathways (MEP) are constructed accordingly.

3. Results and discussion

To study the capture zone for O₂ adsorption and supply, we first calculated whether O₂ can bond on the perfect CeO₂. As discussed in the previous studies [4,6], O₂ is weakly adsorbed on both CeO₂(1 1 1) and (1 1 0) surfaces (−0.07–0.02 eV for (1 1 1) and 0.01–0.03 eV for (1 1 0), see Scheme 1 and Table 1), whereas a stronger adsorption of O₂ on an oxygen vacancy is obtained (1.86 eV for (1 1 1) and 2.28 eV for (1 1 0), also see Table 1). In spite of O₂ is more liable to adsorb on the O vacancy, it is interesting to find that if an O₂ adsorb on the vacancy (vacancy is healed); further O₂ adsorption is not possible. Our results indicate that both perfect CeO₂ and the surface with O vacancies cannot supply O₂ for CO oxidation. The vibrational frequencies are also calculated. The predicted frequencies of selected O₂ adsorption are 1283–1325 and 1205–1230 cm^{−1} for hydroxylated (1 1 1) and (1 1 0) surfaces, respectively, which could be characterized to superoxide species. The frequency of adsorbed O₂ at O vacancy is calculated to be 851–897 cm^{−1}, which is assigned to peroxide species. The results are consistent with the experimental data [5] and allow us to



Scheme 1. The four possible coordination configurations of adsorbed dioxygen species.

Table 1

Calculated adsorption energies with different configurations (see Scheme 1) of O₂ adsorption on the (1 1 1) and (1 1 0) surfaces with respect to the OH coverages.

Surface	Species/ML	0	0.25	0.5	0.75	1	O vacancy
(1 1 1)	End-on	0.01	0.13(1325) ^a	0.15	0.22	0.35	1.86(897)
	Side-on	0.02	0.24(1283)	0.28	0.26	0.47	
	Bridge	−0.07	0.01	0.08	0.05	0.18	
(1 1 0)	End-on	0.03	0.73(1205)	0.92	0.75	1.1	2.28(851)
	Side-on	0.02	0.73(1230)	0.86	0.59	0.94	
	Bridge	0.01	0.54	0.69	0.70	0.73	

^a The values in parentheses are calculated vibrational frequencies of the adsorbed O₂.

identify which species as the key factors in controlling oxidation reactions.

Moisture (water) certainly exists in the catalytic systems. It is widely accepted that H₂O can readily dissociate on the O vacancy of the CeO₂ surface to form two hydroxyl groups [30]. This means that in order to understand the water effect, one should study OH groups on noble-metal/CeO₂. Thus, we study the O₂ adsorption and diffusion on CeO₂(1 1 1) and (1 1 0) surface in the presence of OH. Many possible geometries of O₂ adsorption were calculated. As shown in Table 1, the most stable structure is that O₂ binds over Ce atom with side-on and end-on configuration for the (1 1 1) and (1 1 0) surfaces, respectively, near the OH group with 1/4 ML OH coverage. The adsorption energies are 0.24 and 0.73 eV for the (1 1 1) and (1 1 0) surfaces, respectively. The water concentration may dramatically affect the reactivity. It is, therefore, to understand whether and how the coverage of OH group influences O₂ adsorption. Fig. 1 depicts the adsorption energies of O₂ at different coverage (1/4–1 ML) of OH group. It is evident that the O₂ adsorption energy increases considerably with the concentration of OH group. It is interesting that O₂ cannot adsorb on the perfect CeO₂, but it can adsorb on the O vacancy of defect CeO₂ with the chemisorptions of 1.86 eV (2.28 eV for (1 1 0) surface). However, the O₂ is more likely to diffuse to the vacancy to bind on the defect [4], while OH groups will block O vacancies but allow O₂ adsorption on CeO₂.

We have showed that O₂ can adsorb on the CeO₂ surface in the presence of OH group. If the O₂ supply indeed originates from O₂ adsorption on the CeO₂ surface, then two issues must be

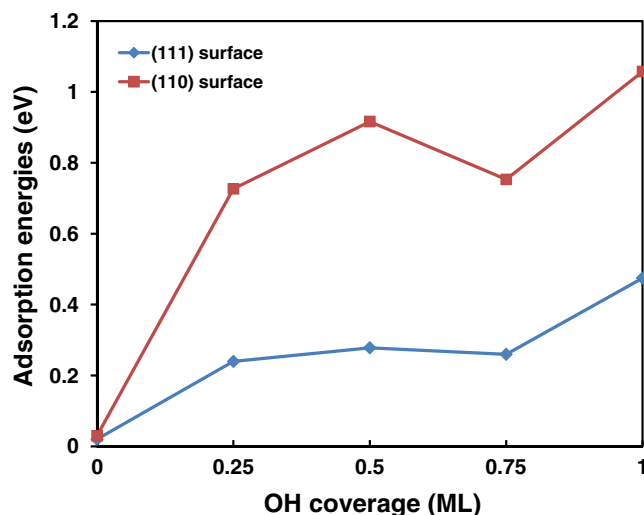


Fig. 1. The calculated O₂ adsorption energies with respect to four different OH coverages.

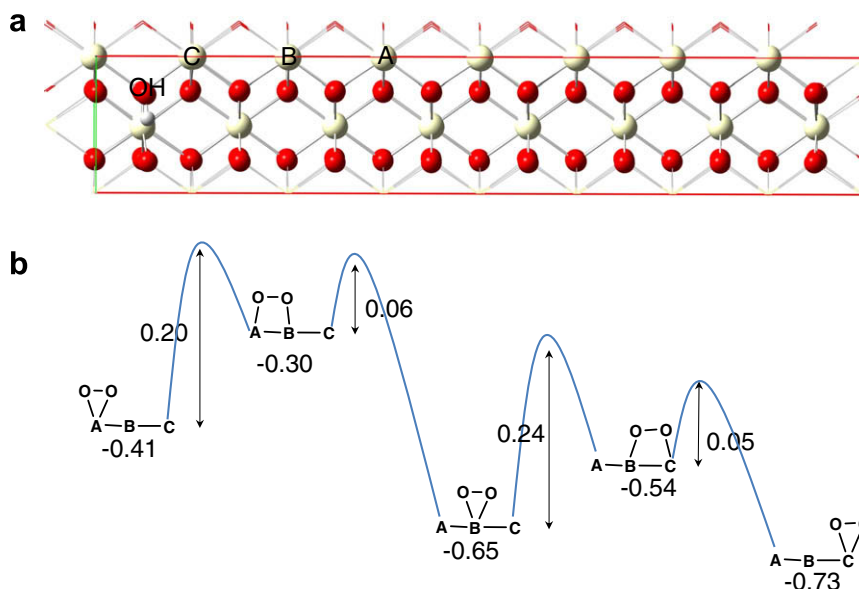


Fig. 2. (a) The top view of the CeO₂(1 1 0) surface in the presence of an OH group. (b) The potential energy profiles and geometries of O₂ diffusion along the Ce atoms from site A to site C. The red, white, and gray balls represent O, Ce, and H atoms, respectively. (For interpretation of the references in colour in this figure legend, the reader is referred to the web version of this article.)

addressed: (i) is the OH effect on the O₂ adsorption long-ranged? (ii) How does O₂ diffuse to the active interfacial region? To further examine the effect of OH group, we study how far the OH group can stabilize the O₂ adsorption on the CeO₂. We employed a rather long supercell, $p(1 \times 8)$ (1 1 0) surface, see Fig. 2a, and O₂ was placed on the sites with different distances from the OH group. The calculated adsorption energies of O₂ on all the sites are shown in Table 2. It is intriguing that O₂ can adsorb on the surface Ce atoms even with a distance over than 10 Å. This result clearly demonstrates that the OH group on CeO₂ surface possesses a long-range effect on the O₂ adsorption. In addition, it should be mentioned that we have also performed calculations for O₂ adsorption on a rather broad supercell, $p(2 \times 4)$ (1 1 0) surface. It is shown that the one row of the unit cell is sufficient due to the difference in the calculated adsorption energies is negligible (less than 0.1 kcal/mol).

As mentioned as above, CO oxidation occurs at the interface of noble-metal/CeO₂. It is critical to have enough O₂ at the interface, which may be supplied by direct O₂ adsorption from the gas. To address this question, we thoroughly study whether O₂ can diffuse on the CeO₂(1 1 0) surface. The pathway with lowest energy is illustrated in Fig. 2. The structure with the O₂ side-on the A site is considered as the initial state of the adsorbed O₂ diffusion. First the adsorbed O₂ migrates to bridge A–B site with a barrier of 0.20 eV. Second the adsorbed O₂ on bridge A–B site overcomes slightly small barrier of 0.06 and diffuses to bind at site B. Similarly, the adsorbed O₂ at site B can diffuse to bond with the Ce at site C. The barriers of this stepwise are 0.24 and 0.05 eV, respectively. Repeating these steps gives rise to the adsorbed O₂ diffusion. It is clear that the adsorbed O₂ can diffuse easily along the Ce atoms of the surface in the presence of OH group. We believe that this may be considered as an O₂ supply to the interface and is very crucial for CO oxidation on the noble-metal/CeO₂. To understand the scenario

of OH group effect on the O₂ adsorption, we also carry out the bader charge calculations. Our calculations show that upon O₂ adsorption on the surface Ce atoms of CeO₂(1 1 0), the excess electrons will be transferred from the surface Ce atoms to O₂ adsorbate. It can be seen in Table 2, O₂ can reversibly abstract electrons from the surface. The large change of charge on the O₂ (−0.766 |e|) is on the site of the nearest to the OH group.

4. Conclusion

In summary, our results demonstrate that O₂ can adsorb on the CeO₂ surface in the presence of OH groups even at low coverages. The OH groups possess a long-range and coverage effects on the O₂ adsorption. We have also identified that the adsorbed O₂ (superoxide) can readily diffuse along the surface Ce atoms in the presence of OH groups, which is a large O₂ supply for CO oxidation on the interface of noble-metal/CeO₂. This information about the reaction mechanism, the catalytic activity of various surface sites, and the relevance of the surface structure would be otherwise difficult to achieve with experimental measurements, indicating that periodic DFT + *U* calculations might play a vital role in the rational explanation of water effects in heterogeneous catalysis.

Acknowledgements

H.-T. Chen would like to acknowledge the (1) National Science Council, Republic of China (Grant Number NSC 97-2113-M-492-001-MY2 and NSC 98-2113-M-034-002-MY2), Chinese Culture University, and Taiwan National Center for Theoretical Sciences (NCTS) for the financial support, and (2) National Center for High-Performance Computing, Taiwan, for the computer time and facilities. In addition, we are deeply indebted to Professor M.C. Lin (from NCTU, Taiwan, and Emory University, USA) for persistent encouragement and instruction.

Appendix A. Supplementary material

Supplementary data associated with this article can be found, in the online version, at doi:10.1016/j.cpl.2010.05.053.

Table 2

Calculated adsorption energies and bader charges with different distances between O₂ and OH using $p(1 \times 8)$ unit cell (1 1 0) surface.

Distances (Å)	2.472	5.898	9.638	13.461
Adsorption energies (eV)	0.73	0.65	0.41	0.34
O ₂ charge (e)	−0.766	−0.621	−0.618	−0.612

References

- [1] M. Valden, X. Lai, D.W. Goodman, *Science* 281 (1998) 1647.
- [2] A. Trovarelli, *Catalysis by Ceria and Related Materials*, Imperial College Press, London, 2002.
- [3] J. Guzman, S. Carrettin, A. Corma, *J. Am. Chem. Soc.* 127 (2005) 3286.
- [4] H.-T. Chen, J.-G. Chang, H.-L. Chen, S.-P. Ju, *J. Comput. Chem.* 30 (2009) 2433.
- [5] V.V. Pushkarev, V.I. Kovalchuk, J.L. d'Itri, *J. Phys. Chem. B* 108 (2004) 5341.
- [6] Y.M. Choi, H. Abernathy, H.-T. Chen, M.C. Lin, M. Liu, *ChemPhysChem* 7 (2006) 1957.
- [7] M. Huang, S. Fabris, *Phys. Rev. B* 75 (2007) 081404(R).
- [8] O. Pozdnyakova-Tellingner, D. Teschner, J. Kröhnert, F.C. Jentoft, A. Knop-Gericke, R. Schlögl, A. Wootsch, *J. Phys. Chem. C* 111 (2007) 5426.
- [9] R. Rajasree, J.H.B.J. Hoebink, J.C. Schouten, *J. Catal.* 223 (2004) 36.
- [10] P.E. Blöchl, *Phys. Rev. B* 50 (1994) 17953.
- [11] G. Kresse, D. Joubert, *Phys. Rev. B* 59 (1999) 1758.
- [12] G. Kresse, J. Hafner, *Phys. Rev. B* 47 (1993) 558.
- [13] G. Kresse, J. Hafner, *J. Phys. Condens. Matter* 6 (1994) 8245.
- [14] G. Kresse, J. Hafner, *Phys. Rev. B* 49 (1994) 14251.
- [15] G. Kresse, J. Furthmüller, *Comp. Mater. Sci.* 6 (1996) 15.
- [16] G. Kresse, J. Hafner, *Phys. Rev. B* 54 (1996) 11169.
- [17] J.P. Perdew, J.A. Chevary, S.H. Vosko, K.A. Jackson, M.R. Pederson, D.J. Singh, C. Fiolhais, *Phys. Rev. B* 46 (1992) 6671.
- [18] J.A. White, D.M. Bird, *Phys. Rev. B* 50 (1994) 4954.
- [19] H.J. Monkhorst, J.D. Pack, *Phys. Rev. B* 13 (1976) 5188.
- [20] S.L. Dudarev, G.A. Botton, S.Y. Savrasov, C.J. Humphreys, A.P. Sutton, *Phys. Rev. B* 57 (1998) 1505.
- [21] M. Huang, S. Fabris, *J. Phys. Chem. C* 112 (2008) 8643.
- [22] M. Nolan, S.C. Parker, G.W. Watson, *Phys. Chem. Chem. Phys.* 8 (2006) 216.
- [23] D.A. Andersson, S.I. Simak, B. Johansson, I.A. Abrikosov, N.V. Skorodumova, *Phys. Rev. B* 75 (2007) 035109.
- [24] C. Loschen, J. Carrasco, K.M. Neyman, F. Illas, *Phys. Rev. B* 75 (2007) 035115.
- [25] D. Mei, N.A. Deskins, M. Dupuis, Q. Ge, *J. Phys. Chem. C* 112 (2008) 4257.
- [26] E.A. Kummerle, G. Heger, *J. Solid State Chem.* 147 (1999) 485.
- [27] A. Ulitsky, R. Elber, *J. Chem. Phys.* 92 (1990) 1510.
- [28] G. Mills, H. Jónsson, G.K. Schenter, *Surf. Sci.* 324 (1995) 305.
- [29] G. Henkelman, B.P. Uberuaga, H. Jónsson, *J. Chem. Phys.* 113 (2000) 9901.
- [30] M.B. Watkins, A.S. Foster, A.L. Shluger, *J. Phys. Chem. C* 111 (2007) 15337.